Article

Electrospun Sericin/PNIPAM-Based Nano-Modified Cotton Fabric with Multi-Function Responsiveness

Jia Li [1,2,3], Bo-Xiang Wang [2,3], De-Hong Cheng [2,3], Zhi-Mei Liu [3], Li-Hua Lv [1], Jing Guo [1,4,*] and Yan-Hua Lu [2,3,*]

1   School of Textile and Material Engineering, Dalian Polytechnic University, Dalian 116034, China;
    lj18840597623@163.com (J.L.); lvlh@dlpu.edu.cn (L.-H.L.)
2   Liaoning Provincial Key Laboratory of Functional Textile Materials, Eastern Liaoning University,
    Dandong 118000, China; bxwang0411@163.com (B.-X.W.); chengdehongldxy1@163.com (D.-H.C.)
3   School of Chemical Engineering, Eastern Liaoning University, Dandong 118003, China; 13842507319@126.com
4   Liaoning Engineering Technology Research Center of Function Fiber and Its Composites,
    Dalian Polytechnic University, Dalian 116034, China
*   Correspondence: guojing8161@163.com (J.G.); yanhualu@aliyun.com (Y.-H.L.); Tel.: +86-137-0409-1879 (J.G.);
    +86-159-4253-2087 (Y.-H.L.)

Abstract: There is a significant interest in developing environmentally responsive or stimuli-responsive smart materials. The purpose of this study was to investigate multi-function responsive cotton fabrics with surface modification on the nanoscale. Three technologies including electrospinning technology, interpenetrating polymer network technology, and cross-linking technology were applied to prepare the multi-function sericin/poly(N-isopropylacrylamide)/Poly(ethylene oxide) nanofibers, which were then grafted onto the surfaces of cotton textiles to endow the cotton textiles with outstanding stimuli-responsive functionalities. The multi-function responsive properties were evaluated via SEM, DSC, the pH-responsive swelling behavior test and contact angle measurements. The results demonstrate that with this method, multi-function responsive, including thermo- and pH-responsiveness, cotton fabrics were fast formed, and the stimuli-responsiveness of the materials was well controlled. In addition, the antimicrobial testing reveals efficient activity of cotton fabrics with the sericin/PNIPAM/PEO nanofiber treatments against Gram-positive bacteria and Gram-negative bacteria such as *Staphylococcus aureus* and *Escherichia coli*. The research shows that the presented strategy demonstrated the great potential of multi-function responsive cotton fabrics fabricated using our method.

Keywords: sericin; poly(N-isopropylacrylamide); cotton fabrics; electrospinning

1. Introduction

Textiles are versatile materials composed of natural or synthetic fibers, with a wide range of applications [1,2]. With the global economy and technological advancements, smart textiles [3–5] are one of the research hotspots in the field of textiles and garments. Intelligent textiles are a sort of smart fabric or material which can be responsive to the external environment or an outside stimulus in behavior, including electrical, chemical, biological agents or physical temperature [6,7]. Currently, in order to introduce some kind of advanced function or special performance, smart textile materials are often modified by direct coating technology such as roll coating, the spraying method or deposition and surface treatment approaches, such as plasma treatment technology, ultraviolet irradiation [8], etc. These technologies are very useful and applied for smart textiles in improving or introducing some kind of certain performance based on the concrete requirements in actual applications. However, it should be mentioned that the utilization of traditional coating technology often inevitably hides the original capabilities of fabrics. Additionally, surface process techniques often concern a complicated process or environmental pollution along with surface structure destruction. This inevitably leads to the degeneration of some other characteristics of fabrics, such as tenderness, breathability and hygroscopicity.

As a comparison, electrospinning technology [9] has shown enormous potential such as filtration, separation [10,11], drug delivery of biomedical materials [12,13] and intelligent fabric modification because of great advantages such as the smaller fiber diameter, the higher porosity and permeability rate, large specific surface area, and high mechanical capacity [14,15], as well as its effective approaches of synergizing the required functions of materials and outstanding performance of textiles. However, the fabrics of intelligent modification with electrospinning technology are generally e-textiles and pressure-sensitive fabrics [16,17]. Furthermore, the fabrics of intelligent modification with electrospinning technology are generally e-textiles [18] and pressure-sensitive fabrics [19]. Though coupling electrospinning technology to thermo-responsive polymers such as poly(N-isopropylacrylamide) can effectively produce smart responsive nanofibers [20–23], few studies use them to modify textiles. In addition, most thermo-responsive textiles are conducted by coating smart polymers in industrial technologies. Currently, the coating smart polymers are mainly prepared and applied in the form of three-dimensional hydrogels with the shortcoming of smaller poriness and lower surface area and response rate.

In our previous work [24], multifunctional mulberry silk fabrics were successfully prepared with PNIPAM/chitosan/PEO nanofibers. The modified mulberry silk fabrics represented brilliant temperature- and pH-susceptivity and antibacterial capabilities. This prompted us to investigate other fabric applications such as cotton fabrics. Based on this, we chose the sericin of the Antheraea pernyi silks as the main raw materials. This took full advantage and improved the application of Antheraea pernyi silk sericin.

Here, we present a strategy for the fabrics, which brings some new ideas of modified fabrics. First, we prepared a kind of thermo-responsive polymer hydrogel by blending sericin/PEO solutions with N-isopropylacrylamide using an interpenetrating polymer network technology. Second, we prepared thermo-responsive nanofiber materials through electrospinning technology. Third, the modified cotton textiles that possessed temperature- and pH-sensitivity were produced by using the nanofiber network. The properties of the smart textiles were investigated and contrasted with those of the other samples. In addition, the biological property of smart textiles was examined with an antimicrobial activity test. This study suggests the potential of the temperature- and pH-responsive smart textiles to tissue engineer support materials, medicine slow release materials and other responsive materials.

2. Experimental Procedure

2.1. Materials

The raw materials (*Antheraea pernyi* silk cocoons, Liaoning Tussah Silk Institute Co., Ltd., Dandong, China) were applied to prepare the regenerated sericin (SS). N-isopropylacrylamide (NIPAM, 98%, Aladdin Reagent, Shanghai, China), N,N,N',N'-tetramethylethylenediamine (TEMED, 99%, Aladdin Reagent, Shanghai, China), ammonium peroxodisulfate (APS, Sinopharm Chemical Reagent Co., Ltd., Shanghai, China) and glutaric dialdehyde (GA, 25%, Kermel Reagent, Tianjin, China) were all analytical grade and used without further purification. Poly(ethylene oxide) (PEO, Mw = 400,000 Da, Shanghai, China) was used without further purification.

2.2. Preparation of the Sericin/PNIPAM/PEO Composite Spinning Solution

Antheraea pernyi is a wild nonmulberry silkworm species, which is a protein fiber and composed of fibroin and sericin [25]. Antheraea pernyi silks were considered increasingly for the textile and apparel industries [26] and medical applications [27] in recent years for their excellent mechanical properties and biocompatibility. As previously reported, regenerated sericin (SS) was extracted from *Antheraea pernyi* raw silk cocoons by using LiBr extractive technique [28]. Then, the regenerated sericin and PEO were dissolved in water under continuous magnetic stirring at 80 °C to prepare a mixed solution. The concentrations of sericin and PEO were 6 wt.% and 15 wt.%, respectively. The monomer

solution (6.5 wt.%) was produced by putting the NIPAM monomer in distilled water and the initiator agent (APS) was all mixed with the above sericin/PEO solution, respectively. Then, the sericin/PNIPAM/PEO interpenetrating network blending spinning solution was prepared by adding TEMED in an as-prepared mixed solution and stirred at 40 °C for 1 h. The concentration values of the sericin, PEO and NIPAM were chosen by our early investigator's literature [24,29]. The formulations, conductivity and surface tension of blending solution is shown in Tables 1 and 2, respectively. The HAAKE RheoStress 1 rheometer (25 mm diameter plate with 1 mm gap) was used to estimate the blending spinning solution viscosity at room temperature under the increasing shear rate from 2 to 100 s^{-1} (see Figure 1).

Table 1. The formulations of the interpenetrating network blending spinning solution.

Code	Sericin: NIPAM: PEO (Volume Ratio)	Sericin (mL)	NIPAM (mL)	PEO (mL)	APS (mg)	5%TEMED (uL)
1	25/45/30	5	9	6	1.36	27.2
2	40/30/30	4	3	3	0.45	9.1
3	55/15/30	11	3	6	0.45	9.1

Table 2. The conductivity and surface tension of the interpenetrating network blending spinning solution.

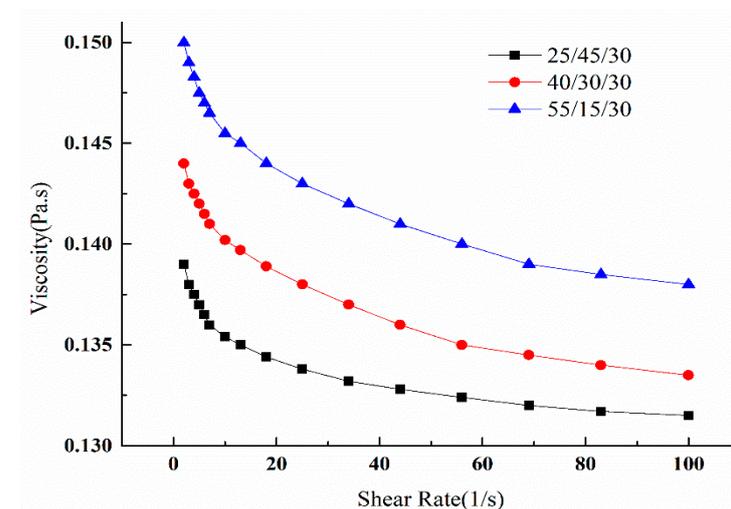| Code	Sericin: NIPAM: PEO (Volume Ratio)	Conductivity (mS/cm)	Surface Tension (mN/m)
1	25/45/30	0.64 ± 0.15	43.5 ± 0.15
2	40/30/30	0.84 ± 0.15	47.7 ± 0.17
3	55/15/30	0.96 ± 0.12	46.4 ± 0.20

Figure 1. Viscosity of the interpenetrating network blending spinning solution.

2.3. Fabrication of Electrospun Sericin/PNIPAM/PEO Nanofibers and Functionalization of Cotton Fabric

Cotton fabric was pretreated by putting it into ultrasonic cleaners which contain distilled water for 0.5 h at room temperature and then dried in the air. The primary sericin/PNIPAM/PEO spinning solutions were loaded into a syringe equipped with a 0.5 mm diameter metal needle and electrospun on the prepared cotton fabric using an electrospinning machine. The functional cotton fabric was prepared by putting the above cotton fabric with nanofibers on the airtight container with glutaraldehyde vapor at room temperature for 24 h for the further cross-linking. The glutaraldehyde showed adequate

safety, having been well applied in the field of biological medicinal materials [30,31]. The illustration of the functional cotton fabric is shown in Figure 2.
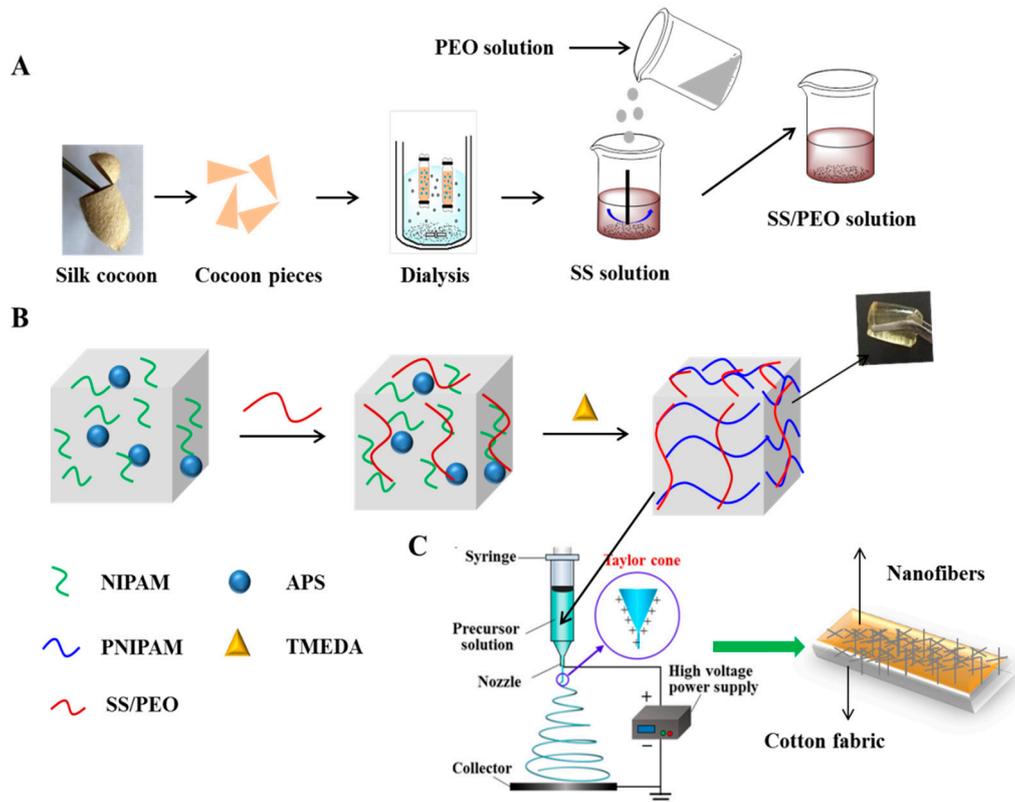

Figure 2. Schematic illustration of the (**A**) fabrication and (**B**) preparation of multifunctional cotton fabric.

The machine (KH08, Jinan, China) was purchased from Jinan Liangrui Technology Co., which had a high voltage direct current (HVDC) and a syringe pump. It was used to prepare the electrospun nanofibers. In this work, all of the electrospinning process was performed at 65% relative humidity (RH), room temperature. The electrospinning parameters are shown as follows: applied voltage 30 kV, working distance 15 cm and flow rate 0.03 mL/h. The parameters for the electrospinning experiments were chosen by our early investigator's literature [24,29]. The nanofibers were deposited at about 1 h and obtained the mats.

2.4. Characterization

2.4.1. Scanning Electron Microscopy

The microstructure of the nanofiber mats and cotton fabric was studied by scanning electron microscope (JSM-IT100, JEOL Ltd., Tokyo, Japan) with acceleration of voltage 20 KV. Before the imaging process, all the samples were sputter-coated with gold.

2.4.2. Fourier Transform Infrared Spectroscopy

Fourier transform infrared spectroscopy (FT-IR, Tensor-37, Bruker, Berlin, Germany) was used to determine the characteristics of the microstructure of NIPAM, sericin, PNIPAM, sericin/PNIPAM/PEO nanofibers and the functionalized cotton fabric with the KBr technique at wavelengths ranging between 400 cm^{-1} and 4000 cm^{-1}. The samples were obtained in a vacuum dryer for 4 h before acquiring the spectra.

2.4.3. Differential Scanning Calorimetry

Differential scanning calorimeter (DSC 7, Perkin Elmer, Waltham, MA, USA) was applied to evaluate thermal behaviors of untreated cotton fabric and functionalized cotton fabric under nitrogen with the flow rate at about 20 mL/min. The swollen sample weight was about 10 mg. The above samples were put in the aluminum sample holder and frozen below $-20\,^\circ$C. The samples were operated at 0–50 $^\circ$C, 2 $^\circ$C min^{-1}. The samples performed heating/cooling cycles three times.

2.4.4. Contact Angle Measurements

Static water contact angle tests were accomplished by using a drop shape analyzer (PT-705, Shanghai, China) with the needle method at flow rate of 1.0 μLs^{-1} in 16% of relative humidity and temperature ranging from 15 $^\circ$C to 45 $^\circ$C. The Young Laplace drop profile fitting method was applied to evaluate the static contact angle results. The needle specification is shown as follows: diameter 0.5 mm and the water droplet volume ~5 μL. The standard deviation of the measurement series might create the error bars.

2.4.5. pH-Responsive Swelling

Sericin is an inherently weak amphipathic polyelectrolyte with the acidic side and alkaline side base, which makes it sensitive to pH [32,33]. The swelling behaviors of sericin/PMIPAM/PEO hydrogels were conducted within a variety of pH values (1.0~11.0), in view of the crucial aspect of the parameters in responsiveness.

In order to determine the swelling ratio, the dried samples were immersed in various pH buffers for 24 h in the temperature 15 $^\circ$C and 37 $^\circ$C that completes with the hydrogels' low critical solution temperature range. Before swollen sample mass testing, it was necessary to remove the surface water of specimens. The average of five samples was used to obtain the final results. The swelling ratio (SR) was calculated as follows [34]:

$$SR(\%) = [(W_t - W_d)/W_d] \times 100 \tag{1}$$

where W_t and W_d are the masses of the swollen sample and dried sample, respectively.

2.4.6. Antimicrobial Activity Measurements

The antibacterial activity of samples was investigated against Gram-positive bacteria and Gram-negative bacteria such as *Staphylococcus aureus* and *Escherichia coli* on the basis of the AATCC 100 test method and GB/T 31713-2015. Before the assay, all samples were made into small pieces at about 0.5×0.5 cm^2. Additionally, UV exposure was applied to sterilize the above samples at about 30 min. The above samples were put, respectively, in the bacterial suspension by using sterile forceps and then immersed in a flask including phosphate-buffered saline at 0.3 mM/70 mL. The phosphate-buffered saline consisted of monopotassium phosphate and the cell culture solution. The cell concentration was about 1×10^5–4×10^5 (CFU)/mL. We shook the above flask on a rotary shaker at 150 rpm, 24 $^\circ$C, 1 h. The 0.5 mL of culture solution was obtained, respectively, from incubated samples before and after shaking for 1 h, and then diluted and placed on the agar plates that were cultivated at 37 $^\circ$C, 1 h. The inhibitory rate (%) was decided as follows [35]:

$$R(\%) = [(B - A)/B] \times 100 \tag{2}$$

where R, B and A were the percentage of bacterial reduction and the bacterial colonies before and after shaking for 24 h, separately.

3. Results and Discussion

3.1. SEM

The surface morphology of the sericin/PNIPAM/PEO nanofibers and functionalized cotton fabric under optimal conditions was decided by SEM (see Figure 3). The final images of the sericin/PNIPAM/PEO nanofibers indicated that the fibers were uniform and contin-

uous without any bead formation (Figure 3a). As shown in Figure 3a, there was breakage in nanofibers when the spinning solution had more NIPAM. The cause might be that the increasing NIPAM caused the bad mechanical properties of nanofibers. This indicates that sericin, NIPAM and PEO were well blended. Based on the morphological analysis of the functionalized cotton fabrics (Figure 3b,c), the sericin/PNIPAM/PEO nanofibers were overlapped and fixed on the surface of the cotton fabric formation bilayer structure. The cross-linked reaction mechanism between sericin and cotton fabric is shown in Figure 3d. The FTIR spectra analysis also confirms the chemical cross-linking reaction of the cotton fabrics and sericin in the presence of glutaraldehyde [36]. The results of SEM showed that the functionalized cotton fabric was also successfully prepared by a combination of electrospinning technology and an interpenetrating polymer network technology.
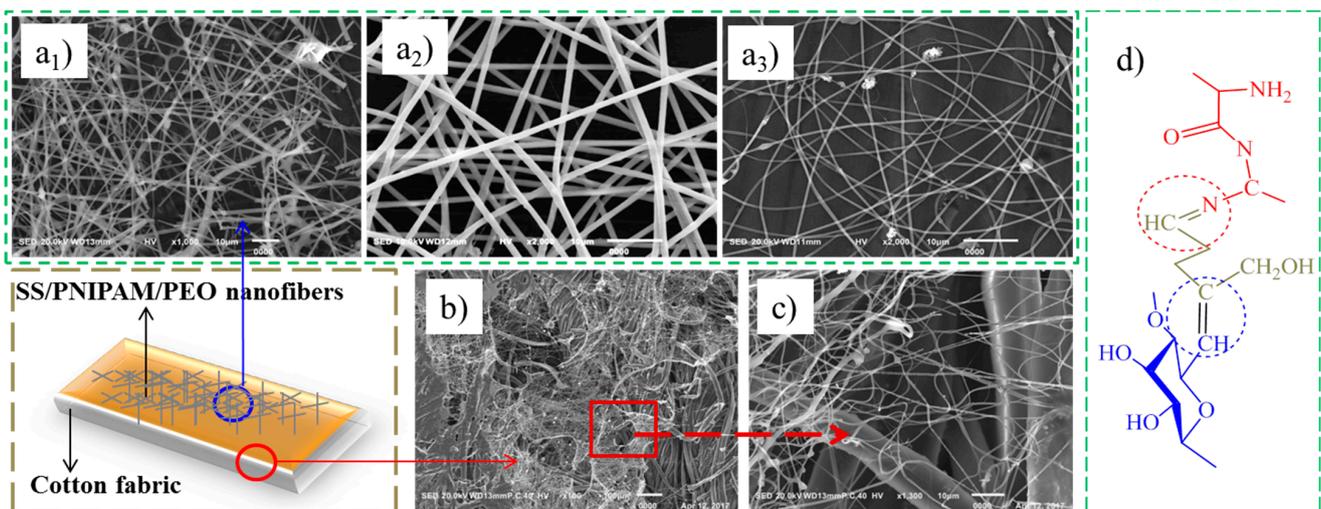

Figure 3. The morphology of (**a**) Sericin/PNIPAM/PEO nanofibers: ((**a₁**) 25/45/30; (**a₂**) 40/30/30; (**a₃**) 55/15/30); (**b**,**c**) Functionalized cotton fabric; (**d**) Reaction mechanism between sericin and cotton.

3.2. FT-IR

Figure 4A presents the Fourier transform infrared spectroscopy of the NIPAM and PNIPAM powders ranging from 2000 cm^{-1} to 1000 cm^{-1}. The disappearance of the 1622 cm^{-1} (–C=C–) peak showed the success of the synthesis of PNIPAM between NIPAM monomers (Figure 4A(a)). The 1652 cm^{-1} connected with the C=O, the 1549 cm^{-1} was related to the C–N stretching vibration and N–H flexural vibration, and the 1245 cm^{-1} corresponded to the C–N–H of PNIPAM [37]. FT-IR was employed to investigate the relationship between sericin/PNIPAM/PEO nanofibers and cotton fabric. The H–C=N– and H–C=C were formed by the crosslinking reaction between GA and sericin and cotton fabric, respectively.

From Figure 4B(e), it could be observed that the characteristic absorption bands at 3084 cm^{-1} could be contributing to the H–C=C group, which proved the cross-linking reaction between the –OH group on cotton and GA. The characteristic band at 1635 cm^{-1} corresponded to the H–C=N– stretching vibration of the modified cotton fabric. This suggested that the cross-linking reaction between the sericin and GA occurred. The –CHO produced a characteristic band at 1713 cm^{-1}. As we know, there was no extra GA in the resulting modified cotton fabric. Thus, the GA could make the reaction with the cotton textiles and sericin, separably. It was indicated that the glutaraldehyde could be a "bridge" that can crosslink the cotton fabric and the nanofibers [33,38].
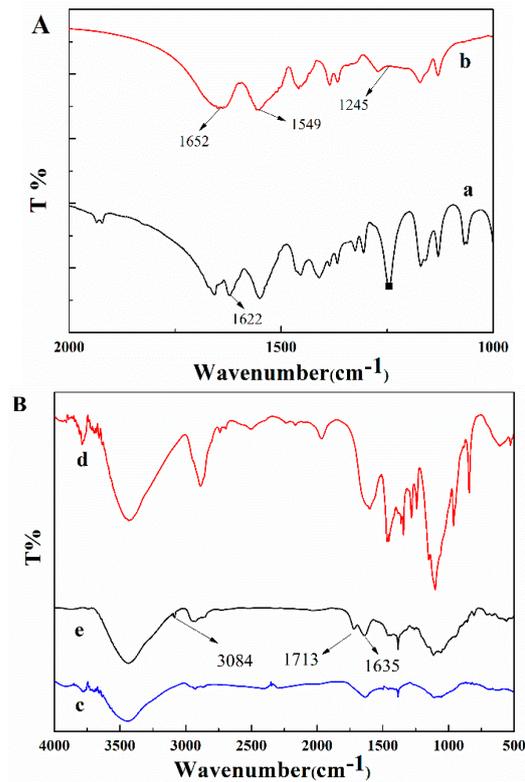
Figure 4. (**A**): The FT-IR spectra (2000–1000 cm^{-1}) of (**a**) NIPAM powders; (**b**) PNIPAM powders; (**B**): The FT-IR spectra (4000–500 cm^{-1}) of (**c**) Sericin/PNIPAM/PEO nanofibers; (**d**) Cotton fabric; (**e**) Functionalized cotton fabric.

3.3. Thermosensitive Behavior

Figure 5A shows the schematic illustration of PNIPAM involving the hydrophobic/hydrophilic transformation. PNIPAM interacted preferentially with water molecules and formed a hydrogen bond in the temperature range below LCST [39]. When increasing the temperature above LCST, PNIPAM molecules gradually turn into hydrogen bonds between polymer molecules. Thus, it was severely restricted for each molecule's mobility because of the hydrogen-bonded polymer network.

The surface wettability of functionalized cotton fabric was measured with different temperatures by using the static contact angle of water droplets (5 μL). Figure 5B exhibits that the static water contact angle of functionalized cotton fabrics increased apparently with the increasing temperature of the fabrics, demonstrating a hydrophilicity/hydrophobicity change of functionalized cotton fabrics. The wettability of functionalized cotton fabrics became a hydrophobic state and the contact angle increased up to the maximum at about 95 ± 1.5°, with the temperature improved.

Figure 5C shows the differential scanning calorimetry (DSC) thermogram curves of modified cotton fabric and cotton fabric. The initial temperature was considered as the lower critical solution temperature (LCST) value that was estimated with the intersection points of the two tangents (see Figure 5). It could be seen that the LCST of nanofibers and modified cotton fabric is 32.03 °C and 34.47 °C, respectively. Additionally, there was no phase transition peak in common cotton fabric. It was shown that the LCST of modified cotton fabric is between 30 °C and 36 °C, close to human body temperature.
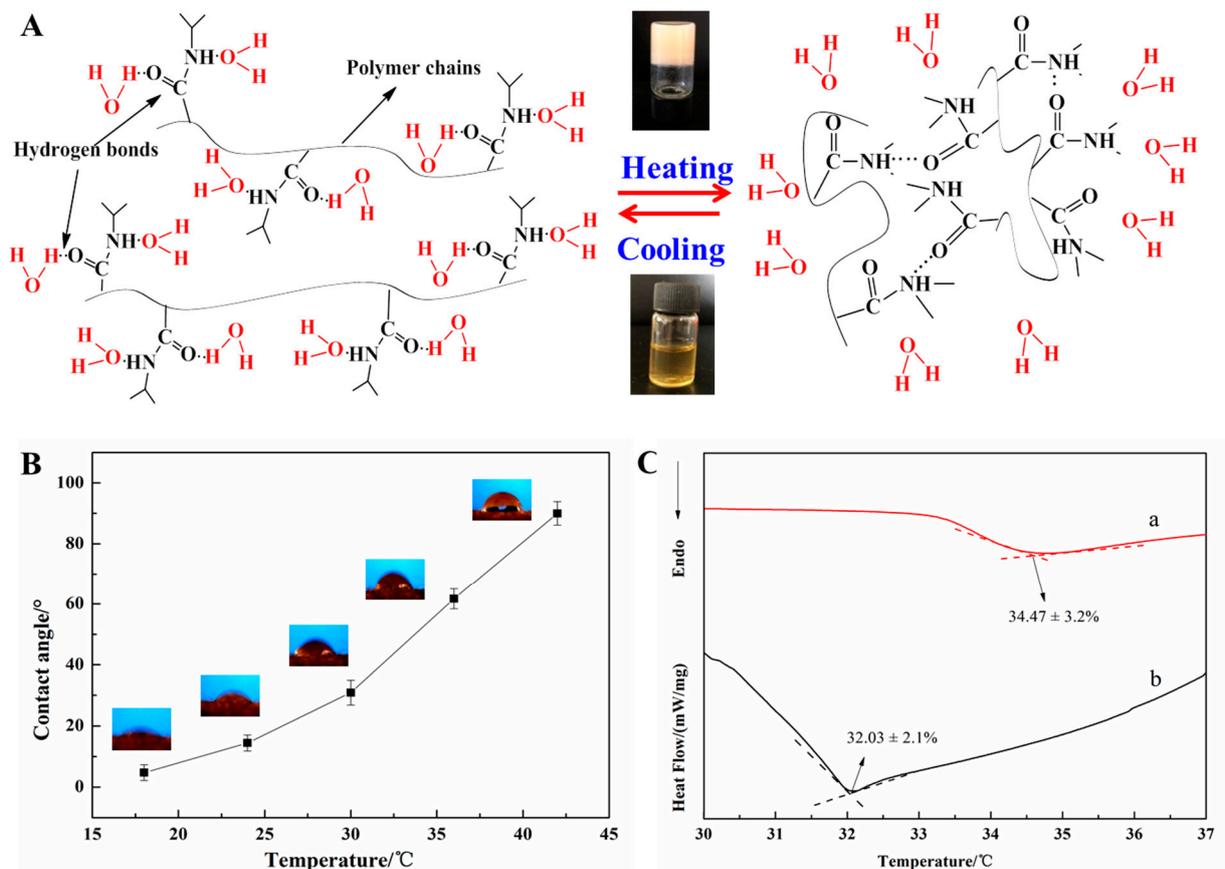
Figure 5. Representation of (**A**) the hydrophobic–hydrophilic phase transition of PNIPAM hydrogels; (**B**) Contact angle measurements of multifunctional cotton fabric at different temperatures; (**C**) Differential scanning calorimetry thermogram curves of modified cotton fabric and cotton fabric. (**a**) Cotton fabric; (**b**) Functionalized cotton fabric. (The final results of data are shown as mean ± standard deviation).

3.4. pH-Responsive Swelling Behaviors

In Figure 6, the images show that sericin/PNIPAM/PEO hydrogels had different swelling ratio changes according to the pH swelling medium at temperatures of 15 °C and 37 °C. From Figure 6, it was shown that all the hydrogels presented the same trends and temperature-sensitive property under the pH test range. The swelling ratio of hydrogels was much higher at 15 °C than at 37 °C, which showed a temperature-sensitive characteristic. This was largely due to the network shrinking of PNIPAM when the temperature of the solutions was above LCST (37 °C). The swelling ratio of sericin/PNIPAM/PEO (55/15/30) hydrogel decreased a little with a rise in temperature. The minimum swelling ratio of hydrogel appeared at about pH 4.0. This is due to the non-charged and hydrophobic form of sericin side chains. The increasing swelling ratios of sericin/PNIPAM/PEO (55/15/30) hydrogel appeared with reducing the pH buffer solutions down to 4.0 or increasing it above 4.0. This was because the $-NH_2$ of sericin was protonated into $-NH_3^+$ and $-COOH$ of sericin charged to $-COO^-$ and then enhanced the electrostatic repulsion of interpenetrating network hydrogels.

The results showed that the swelling ratio was lower in all the specimens at pH 4.0 and pH 8.0, no matter what the composition of the hydrogels was. Additionally, there were better swelling ratios under acid or alkaline conditions.
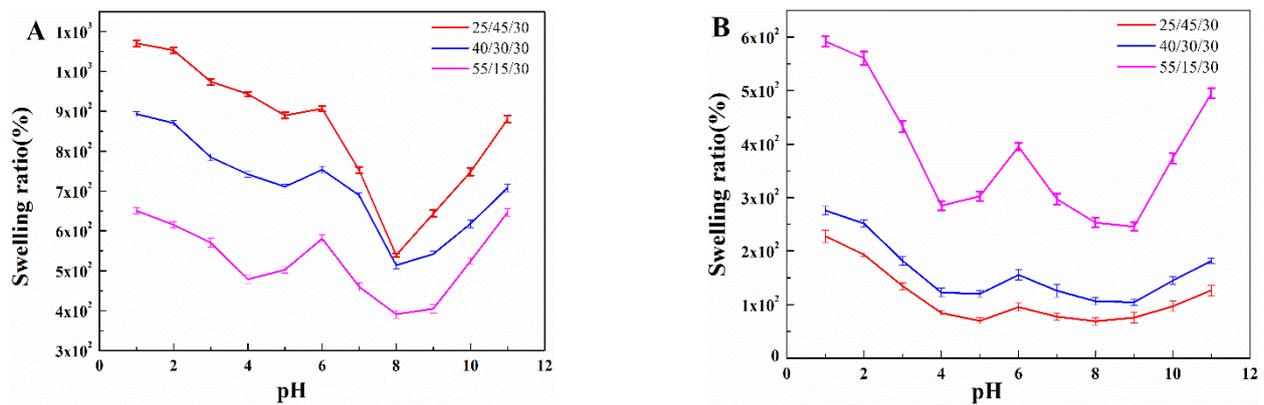
Figure 6. Swelling ratio of sericin/PNIPAM/PEO hydrogels in pH buffer solutions at (**A**) 15 °C and (**B**) 37 °C, the final results of data are shown as mean ± standard deviation.

With the increasing sericin concentration, the swelling ratios increased at 15 °C (Figure 6A), and the order of swelling ratios was a complete transformation at 37 °C (Figure 6B). Along with the increase in sericin content, the number of –COOH and –NH$_2$ was increased and resulted in the enhancement of the electrostatic repulsion of hydrogel. As can be seen, the sericin/PNIPAM/PEO hydrogels showed simultaneous pH and temperature sensitivity. It was an effective way to adjust the equilibrium swelling ratio and the swelling property of the hydrogels by changing the mixed proportion of hydrogels.

3.5. Antimicrobial Activity

The antibacterial activity of samples was evaluated against Gram-positive bacteria and Gram-negative bacteria such as *Staphylococcus aureus* (ATCC 6538) and *Escherichia coli* (ATCC 8739). The antimicrobial capability of the untreated cotton fabric and functionalized cotton fabric is shown in Table 3. The functionalized cotton fabrics exhibited antimicrobial property against the above microorganisms. The sericin/PNIPAM/PEO nanofibers could inhibit the growth of bacteria. All functionalized cotton fabrics showed lower antibacterial efficiency against *E. coli* and higher antibacterial property against *S. aureus*. It was revealed that the antibacterial efficiency of the functionalized cotton fabrics exhibited the highest antibacterial efficiency up to 85% of *E. coli* and 90% of *S. aureus*. This may be due to the fact that the sericin could control the free movement of the bacteria, inhibited respiration and finally rose to the death of bacteria. The sericin molecules had the electrostatic attraction with cell membranes of bacteria. The electrostatic attraction would decrease bacterial conductivity, reduce cell membrane permeability and partially inhibit metabolism. As a result, the intracellular composition containing water and protein was discharged and finally led to the death of bacteria [40].

Table 3. Antibacterial characteristic of cotton fabrics against *S. aureus* and *E. coli* bacteria.

Sample	*E. coli*					*S. aureus*				
	Surviving Cells (CFU/mL)					Surviving Cells (CFU/mL)				
	1	2	3	4	5	1	2	3	4	5
Untreated cotton fabric	251,000	232,000	243,000	235,000	250,000	241,000	234,000	228,000	221,000	230,000
Functionalized cotton fabric	27,000	36,000	26,000	18,000	19,000	5000	7000	9000	14,000	12,000
Reduction(%)	89.24	84.48	89.30	92.34	92.40	97.93	97.01	96.05	93.67	94.78
Mean ± SD			89.55 ± 3.2%					95.89 ± 1.7%		

4. Conclusions

In conclusion, a simple and effective strategy has been designed and proved for the surface modification of cotton textiles with multi-function responsiveness. The multi-function modified cotton fabric showed obvious temperature- and pH responsiveness behavior and antibacterial activity. The swelling ratio decreased significantly under the increasing temperature to the LCST of the hydrogels. The low values of equilibrium swelling ratios appeared at about pH 4.0 and 8.0. This is due to the salting-out effect and the isoelectric point (PI) of SS. The bacterial decline of multi-function modified cotton textiles against *E. coli* and *S. aureus* was all above 89%. Through the different combinations of textiles and smart polymers via electrospinning technology, the strategy shows robust advantages for the preparation of textiles with multi-function responsive properties. Moreover, this is also a simple, rapid and green environmental protection method for the fabrication of multi-functional fabrics. This study may provide the strategy of modified fabrics that can possess environmentally responsive or stimuli-responsive properties and that are supposed to be prospective materials, especially in smart and functional textile applications.

Here, this study is just a first step for the preparation of smart fabrics with nanofibers as a finishing technology. However, we would perform comprehensive functional testing for the real applications. Other applications of sericin/PNIPAM-based nano-modified cotton textiles such as mechanical properties, comfort capabilities and biocompatibility testing, and cell cytotoxicity tests will be shown in the following manuscripts.

Author Contributions: Conceptualization, J.G. and Y.-H.L.; methodology, J.L.; experimentation, J.L., B.-X.W., D.-H.C., and Z.-M.L.; date analysis, J.L. and L.-H.L. supervision, J.L., J.G. and Y.-H.L. All authors have read and agreed to the published version of the manuscript.

Institutional Review Board Statement: Not Applicable.

Informed Consent Statement: Not applicable.

Data Availability Statement: Data is contained within the article.

Conflicts of Interest: The authors declare no conflict of interest.

References

1. Gong, J.; Xu, B.; Tao, X. Three-Dimensionally Conformal Porous Microstructured Fabrics via Breath Fig-ures: A Nature-Inspired Approach for Novel Surface Modification of Textiles. *Sci. Rep.* **2017**, *7*, 1–9.
2. Trovato, V.; Teblum, E.; Kostikov, Y.; Pedrana, A.; Re, V.; Nessim, G.D.; Rosace, G. Electrically conductive cotton fabric coatings developed by silica sol-gel precursors doped with surfactant-aided dispersion of vertically aligned carbon nanotubes fillers in organic solvent-free aqueous solution-ScienceDirect. *J. Colloid Interface Sci.* **2020**, *586*, 120–134. [CrossRef]
3. Zhu, S.; Wang, M.; Qiang, Z.; Song, J.; Wang, Y.; Fan, Y.; You, Z.; Liao, Y.; Zhu, M.; Ye, C. Multi-functional and Highly Conductive Textiles with Ultra-high Durability through 'Green' Fabrication Process. *Chem. Eng. J.* **2020**, *406*, 127140. [CrossRef]
4. Ivanoska-Dacikj, A.; Stachewicz, U. Smart textiles and wearable technologies—Opportunities offered in the fight against pandemics in relation to current COVID-19 state. *Rev. Adv. Mater. Sci.* **2020**, *59*, 487–505. [CrossRef]
5. Martínez-Pérez, C.A. Electrospinning: A promising technique for drug delivery systems. *Rev. Adv. Mater. Sci.* **2020**, *59*, 441–454. [CrossRef]
6. Huang, Z.S.; Shiu, J.W.; Way, T.F.; Rwei, S.P. A Thermo-Responsive Random Copolymer of Poly(NIPAm-co-FMA) for Smart Textile Applications. *Polymers* **2019**, *184*, 121917. [CrossRef]
7. Kreuzer, L.P.; Widmann, T.; Hohn, N.; Wang, K.; Bießmann, L.; Peis, L.; Moulin, J.F.; Hildebrand, V.; Laschewsky, A.; Papadakis, C.M. Swelling and Exchange Behavior of Poly(sulfobetaine)-Based Block Copolymer Thin Films. *Macromolecules* **2019**, *52*, 3486–3498. [CrossRef]
8. Tao, X. *Handbook of Smart Textiles*; CRC Press: Boca Raton, FL, USA, 2016.

9. Sun, B.; Long, Y.Z.; Zhang, H.D.; Li, M.M.; Duvail, J.L.; Jiang, X.Y.; Yin, H.L. Advances in three-dimensional nanofibrous macrostructures via electrospinning. *Prog. Polym. Sci.* **2014**, *39*, 862–890. [CrossRef]

10. Cui, J.; Lu, T.; Li, F.; Wang, Y.; Lei, J.; Ma, W.; Zou, Y.; Huang, C. Flexible and Transparent Composite Nanofibre Membrane that was Fabricated via a "Green" Electrospinning Method for Efficient Particulate Matter 2.5 Capture. *J. Colloid Interface Sci.* **2020**, *582*, 506–614. [CrossRef]

11. Barani, M.; Bazgir, S.; Hosseini, M.K.; Hosseini, P.K. Eco-facile application of electrospun nanofibers to the oil-water emulsion separation via coalescing filtration in pilot- scale and beyond. *Process Saf. Environ. Prot.* **2020**, *148*, 342–357. [CrossRef]

12. Morais, M.; Coimbra, P.; Pina, M. Comparative Analysis of Morphological and Release Profiles in Ocular Implants of Acetazo-lamide Prepared by Electrospinning. *Pharmaceutics* **2021**, *13*, 260. [CrossRef] [PubMed]

13. Luraghi, A.; Peri, F.; Moroni, L. Electrospinning for drug delivery applications: A review. *J. Control. Release* **2021**, *33*, 1–37.

14. Zhu, J.; Jiang, S.; Hou, H.; Agarwal, S.; Greiner, A. Low Density, Thermally Stable, and Intrinsic Flame Retardant Poly(bis(benzimidazo)Benzophenanthroline-dione) Sponge. *Macromol. Mater. Eng.* **2018**, 303. [CrossRef]

15. Park, S.M.; Lee, S.J.; Lim, J.; Kim, B.C.; Han, S.J.; Kim, D.S. Versatile fabrication of size and shape-controllable nanofibrous concave mi-crowells for cell spheroid formation. *ACS Appl. Mater. Interfaces* **2018**, *10*, 37878–37885. [CrossRef]

16. Yang, W.; Gong, W.; Hou, C.; Su, Y.; Guo, Y.; Zhang, W.; Li, Y.; Zhang, Q.; Wang, H. All-fiber tribo-ferroelectric synergistic electronics with high thermal-moisture stability and comfortability. *Nat. Commun.* **2019**, *10*, 1–10. [CrossRef] [PubMed]

17. Zhou, Y.; He, J.; Wang, H.; Qi, K.; Nan, N.; You, X.; Shao, W.; Wang, L.; Ding, B.; Cui, S. Highly sensitive, self-powered and wearable electronic skin based on pressure-sensitive nanofiber woven fabric sensor. *Sci. Rep.* **2017**, *7*, 1–9. [CrossRef]

18. Pawłowska, S.; Rinoldi, C.; Nakielski, P.; Ziai, Y.; Urbanek, O.; Li, X.; Kowalewski, T.A.; Ding, B.; Pierini, F. Ultraviolet Light-Assisted Electrospinning of Core–Shell Fully Cross-Linked P(NIPAAm-co-NIPMAAm) Hydrogel-Based Nanofibers for Thermally Induced Drug Delivery Self-Regulation. *Adv. Mater. Interfaces* **2020**, *7*, 2000247. [CrossRef]

19. Jin, S.; Liu, M.; Zhang, F.; Chen, S.; Niu, A. Synthesis and characterization of pH-sensitivity semi-IPN hydrogel based on hydrogen bond between poly(N-vinylpyrrolidone) and poly(acrylic acid). *Polymer* **2006**, *47*, 1526–1532. [CrossRef]

20. Sengor, M.; Ozgun, A.; Gunduz, O.; Altintas, S. Aqueous electrospun core/shell nanofibers of PVA/microbial transglutaminase cross-linked gelatin composite scaffolds. *Mater. Lett.* **2019**, *263*, 127233. [CrossRef]

21. Nakielski, P.; Pawłowska, S.; Rinoldi, C.; Ziai, Y.; De Sio, L.; Urbanek, O.; Zembrzycki, K.; Pruchniewski, M.; Lanzi, M.; Salatelli, E.; et al. Multifunctional Platform Based on Electrospun Nanofibers and Plasmonic Hydrogel: A Smart Nanostructured Pillow for Near-Infrared Light-Driven Biomedical Applications. *ACS Appl. Mater. Interfaces* **2020**, *12*, 54328–54342. [CrossRef]

22. Guo, J.W.; Wang, C.F.; Lai, J.Y.; Lu, C.H.; Chen, J.K. Poly(N-isopropylacrylamide)-gelatin hydrogel membranes with thermo-tunable pores for water flux gating and protein separation. *J. Membr. Sci.* **2020**, *618*, 118732. [CrossRef]

23. Zheng, X.; Liu, X.; Zha, L. Fabrication of ultrafast temperature-responsive nanofibrous hydrogel with superelasticity and its 'on–off' switchable drug releasing capacity. *J. Appl. Polym. Sci.* **2021**, 138. [CrossRef]

24. Li, J.; Wang, B.; Lin, J.; Cheng, D.; Lu, Y. Multifunctional Surface Modification of Mulberry Silk Fabric via PNI-PAAm/Chitosan/PEO Nanofibers Coating and Cross-Linking Technology. *Coatings* **2018**, *8*, 68. [CrossRef]

25. Malay, A.D.; Sato, R.; Yazawa, K.; Watanabe, H.; Ifuku, N.; Masunaga, H.; Hikima, T.; Guan, J.; Mandal, B.B.; Damrongsakkul, S.; et al. Relationships between physical properties and sequence in silkworm silks. *Sci. Rep.* **2016**, *6*, 27573. [CrossRef] [PubMed]

26. Lu, Y.; Cheng, D.; Lu, S.; Huang, F.; Li, G. Preparation of quaternary ammonium salt of chitosan nanoparticles and their textile properties on Antheraea pernyi silk modification. *Text. Res. J.* **2014**, *84*, 2115–2124. [CrossRef]

27. Varone, A.; Knight, D.; Lesage, S.; Vollrath, F.; Rajnicek, A.M.; Huang, W. The potential of Antheraea pernyi silk for spinal cord repair. *Sci. Rep.* **2017**, *7*, 1–10. [CrossRef]

28. Wang, B.; Zhang, S.; Wang, Y.; Si, B.; Cheng, D.; Liu, L.; Lu, Y. Regenerated Antheraea pernyi Silk Fibro-in/Poly(N-isopropylacrylamide) Thermosensitive Composite Hydrogel with Improved Mechanical Strength. *Polymers* **2019**, *11*, 302. [CrossRef] [PubMed]

29. Li, J.; Wang, B.X.; Cui, Y.F.; Yu, Z.C.; Hao, X.; Huang, F.Y.; Cheng, D.H.; Lu, Y.H. Fabrication and Super-Antibacterial Property of Nanosil-ver/Sericin/Poly(ethylene oxide) Nanofibers through Electrospinning-Combined Postdeposition Method. *J. Nanomater.* **2016**, *2016*, 45. [CrossRef]

30. Pinto, R.V.; Gomes, P.S.; Fernandes, M.H.; Costa, M.E.; Almeida, M.M. Glutaraldehyde-crosslinking chitosan scaffolds reinforced with calcium phosphate spray-dried granules for bone tissue applications. *Mater. Sci. Eng.* **2020**, *109*, 110557. [CrossRef]

31. Valizadeh, S.; Naseri, M.; Babaei, S.; Hosseini, S.M.; Imani, A. Development of bioactive composite films from chitosan and carboxymethyl cellulose using glutaraldehyde, cinnamon essential oil and oleic acid. *Int. J. Biol. Macromol.* **2019**, *134*, 604–612. [CrossRef]

32. Ai, L.; He, H.; Wang, P.; Cai, R.; Tao, G.; Yang, M.; Liu, L.; Zuo, H.; Zhao, P.; Wang, Y. Rational Design and Fabrication of ZnONPs Functionalized Sericin/PVA Antimicrobial Sponge. *Int. J. Mol. Sci.* **2019**, *20*, 4796. [CrossRef]

33. Jahanshahi, M.; Kowsari, E.; Haddadi-Asl, V.; Khoobi, M.; Lee, J.H.; Kadumudi, F.B.; Talebian, S.; Kamaly, N.; Mehrali, M. Sericin grafted multifunctional curcumin loaded fluorinated graphene oxide nanomedicines with charge switching properties for effective cancer cell targeting. *Int. J. Pharm.* **2019**, *572*, 118791. [CrossRef]

34. Wu, W.; Li, W.; Wang, L.Q.; Tu, K.; Sun, W. Synthesis and characterization of pH- and temperature-sensitive silk sericin/poly(N-isopropylacrylamide) interpenetrating polymer networks. *Polym. Int.* **2006**, *55*, 513–519. [CrossRef]

35. Deng, X.; Nikiforov, A.Y.; Coenye, T.; Cools, P.; Aziz, G.; Morent, R.; De Geyter, N.; Leys, C. Antimicrobial nano-silver non-woven polyethylene terephthalate fabric via an atmospheric pressure plasma deposition process. *Sci. Rep.* **2015**, *5*, 10138. [CrossRef] [PubMed]

36. Purwar, R.; Verma, A.; Batra, R. Antimicrobial gelatin/sericin/clay films for packaging of hygiene products. *J. Polym. Eng.* **2019**, *39*, 744–751. [CrossRef]

37. Wang, B.; Wu, X.; Li, J.; Hao, X.; Lin, J.; Cheng, D.; Lu, Y. Thermosensitive Behavior and Antibacterial Activity of Cotton Fabric Modified with a Chitosan-poly(N-isopropylacrylamide) Interpenetrating Polymer Network Hydrogel. *Polymers* **2016**, *8*, 110. [CrossRef] [PubMed]

38. Cui, Y.; Xing, Z.; Yan, J.; Lu, Y.; Xiong, X.; Zheng, L. Thermosensitive Behavior and Super-Antibacterial Properties of Cotton Fabrics Modified with a Sercin-NIPAAm-AgNPs Interpenetrating Polymer Network Hydrogel. *Polymers* **2018**, *10*, 818. [CrossRef]

39. Minier, S.; Kim, H.J.; Zaugg, J.; Mallapragada, S.K.; Vaknin, D.; Wang, W. Poly(N-isopropylacrylamide)-grafted gold nanoparticles at the vapor/water interface. *J. Colloid Interface Sci.* **2021**, *585*, 312–319. [CrossRef]

40. Xue, R.; Liu, Y.; Zhang, Q.; Liang, C.; Qin, H.; Liu, P.; Wang, K.; Zhang, X.; Chen, L.; Wei, Y. Shape Changes and Interaction Mechanism of Escherichia coli Cells Treated with Sericin and Use of a Sericin-Based Hydrogel for Wound Healing. *Appl. Environ. Microbiol.* **2016**, *82*, 4663–4672. [CrossRef]